



Notched Connections for Timber-Concrete Composite Bridges – Investigations on the Fatigue Behaviour

Simon Mönch¹, Ulrike Kuhlmann²

1 Introduction

Based on the combination of timber and concrete, timber-concrete composite bridges (TCC bridges) enable economical bridge constructions. Both materials are used according to their advantageous properties. In the case of typical single-span TCC bridges subjected to bending, the timber cross-section is placed in the tension area and the concrete cross-section in the compression area. In order to allow for high single and distributed loads, connectors between timber and concrete with high strength and stiffness are required.

A notched connection is characterized by very high strength and stiffness as well as an easy manufacturing and therefore is optimal suitable as connection between timber and concrete for TCC road bridges with heavy loads. Thus, notches as TCC shear connectors enable the construction of efficient TCC bridges with large spans. For road bridges, however, the verification of sufficient fatigue strength under frequently recurring traffic loads is required.

In the case of covered wooden bridges, which were built more and more often in Europe from the 13th century and onwards, a roof served as protection against the weather. Figure 1 (left) shows an example of a covered pedestrian bridge over the river Saane near Gümmenen (CH) [1]. Even today there are still many very well preserved covered wooden bridges. For innovative TCC bridges, the concrete deck, which extends sideways over the timber cross-section, acts as structural timber protection (see Figure 1 (right)). Kerbs, roadway expansion joints and railings can be designed by using common constructional details for concrete bridges. The use of timber as a regenerative building material significantly reduces the total weight of the bridge compared to conventional concrete constructions. A high degree of prefabrication of the timber elements also allows for a significant reduction in construction time.



Figure 1: Timber bridge with roof near Gümmenen (CH), built in the 15th century [1] (left) and TCC bridge across the river Agger in Lohmar with 28 m midspan, built in 2014 [2] (right).

Due to their high values of strength and stiffness, notches form ideal connectors between timber and concrete for TCC bridges. Figure 2 shows a notched connection with the relevant geometrical parameters: h_n = notch depth, l_n = notch length, l_v = timber length in front of the notch, h_t = timber thickness, h_c = concrete thickness, α = notch inclination of the edge and screws for preventing uplift.

In this contribution, first an overview of the current state of research is given. Subsequently, experiments on the fatigue behaviour of notched connections on push-out tests are presented, which were conducted among others at the University of Stuttgart in recent years. In the next step, experiments on TCC beams as test specimens measuring 4 m in length are presented, which were performed in 2021. Finally, S-N-curves for the fatigue verification derived from the TCC push-out and beam tests are discussed.

¹ Simon Mönch, Scientific Researcher, University of Stuttgart, Institute of Structural Design, Germany, simon.moench@ke.uni-stuttgart.de

² Ulrike Kuhlmann, Head of Institute, University of Stuttgart, Institute of Structural Design, Germany, sekretariat@ke.uni-stuttgart.de

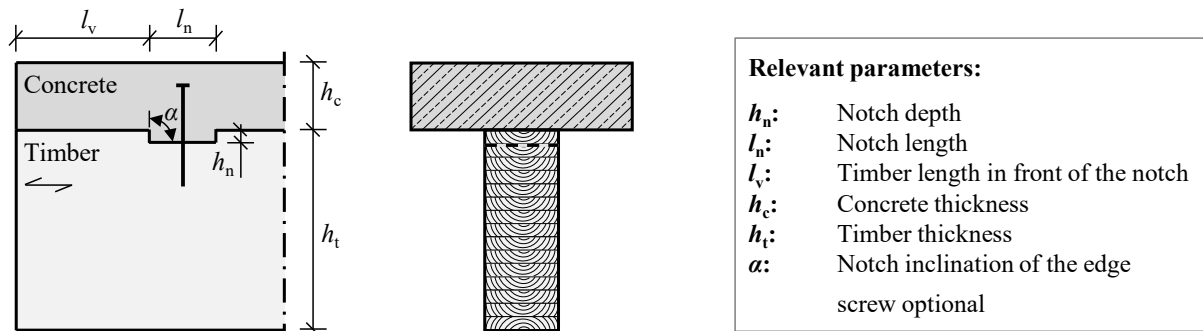


Figure 2: Drawing of a notched connection with geometrical parameters: side view (left) and cross section (right).

2 State of the art

CEN/TS 19103 [3], a European Technical Specification (TS) for the design of timber-concrete composite structures was published in November 2021. This Technical Specification was adopted by the European Committee for Standardization (CEN) in July 2021, and it will be applied as a future standard for provisional application. The aim is to subsequently transfer the CEN/TS into a part of Eurocode 5. Rules in the CEN/TS are partially based on results of extensive static TCC push-out and beam tests with notched connections, carried out by the Institute of Structural Design at the University of Stuttgart in recent years, (see [4] to [8]).

As a result, TCC elements can safely be designed as economical, wide-span slabs for multi-storey and industrial buildings and are already used more often. For TCC bridges (especially subjected to road traffic) this currently applies only to a limited extent. Therefore, a verification of sufficient fatigue strength under frequently recurring traffic loads is required. Currently, design rules for the fatigue verification of TCC bridges and of appropriate connectors are not given in the standard.

In the current version of EN 1995-2, Annex A [9], a fatigue verification for pure timber structures is given. The timber strength is reduced by the coefficient k_{fat} as a function of the number of load cycles. This coefficient also includes the stress ratio R , which is the ratio of the numerically smallest to the numerically largest design stress ($\sigma_{d,min} / \sigma_{d,max}$) due to relevant fatigue loading. At present, it has only been partially investigated to what extent the k_{fat} verification also applies to TCC structures and, in particular, to notches as shear connectors.

Initial tests on notches under cyclic loading were conducted by Kuhlmann & Aldi (2010) [10]. Simon (2008) [11] also conducted a small cyclic test series. However, due to low maximum loads, some run-outs occurred (no failure appeared after more than 2 million load cycles) [11]. The tests were stopped and the results consequently could not be used to derive S-N-curves. However, they showed tendencies to high fatigue strength in the range of low maximum loads.

3 Static and cyclic TCC push-out tests with notched connections

In order to significantly increase the amount of cyclic TCC tests with notched connections and to investigate further parameters, a research project [8] funded by the German Research Foundation (DFG) was realised. Extensive static and cyclic tests with notched connections on 36 push-out test specimens were conducted in a total of 13 test series, over a period of three years (2019-2021) [4], [6]. Based on the push-out tests, 9 TCC beam tests were performed in a total of 3 test series in 2021, results are discussed in section 4.

All test specimens were made of glued-laminated timber out of spruce of quality GL 28h according to EN 14080 [12] and concrete of quality C 30/37 according to EN 1992-1-1 [13]. For all specimens, the notch depth h_n was chosen to 4 cm, which is a common dimension in bridge construction (cf. multi-storey buildings: usually $h_n = 2.0$ cm). The timber length in front of the loaded edge of the notch l_v was always 40 cm (corresponding to $10 \cdot h_n$).

The influence of the notch depth h_n in relation to the timber length in front of the loaded edge of the notch l_v on the failure mode (ductile timber compression failure or brittle timber shear failure in front of the notch, with subsequent cracks in the concrete) has already been investigated in former static test series (see [7]).



In principle, a ductile failure is preferable, because deformations are recognized before fracture. However, to derive S-N-curves from cyclic tests, a clear safe sided failure criterion is needed. In order to achieve a clear brittle timber shear failure, the timber length in front of the loaded edge of the notch was chosen to $10 \cdot h_n$ for all TCC test series within the DFG research project [8].

The results obtained from the static tests, which served as input values for the cyclic test series, focused on the evaluation of values for strength and stiffness of the notched connection (see [4], [6]). Based on this, the number of load cycles before failure (timber shear failure in front of the loaded edge of the notch, see Figure 3 (left and middle)), was determined by means of cyclic push-out tests with single amplitude load spectrum for varied maximum loads F_{\max} . Subsequently, S-N-curves for a stress ratio of $R = 0.1$ were derived together with results from [10] (see Figure 3 (right)).

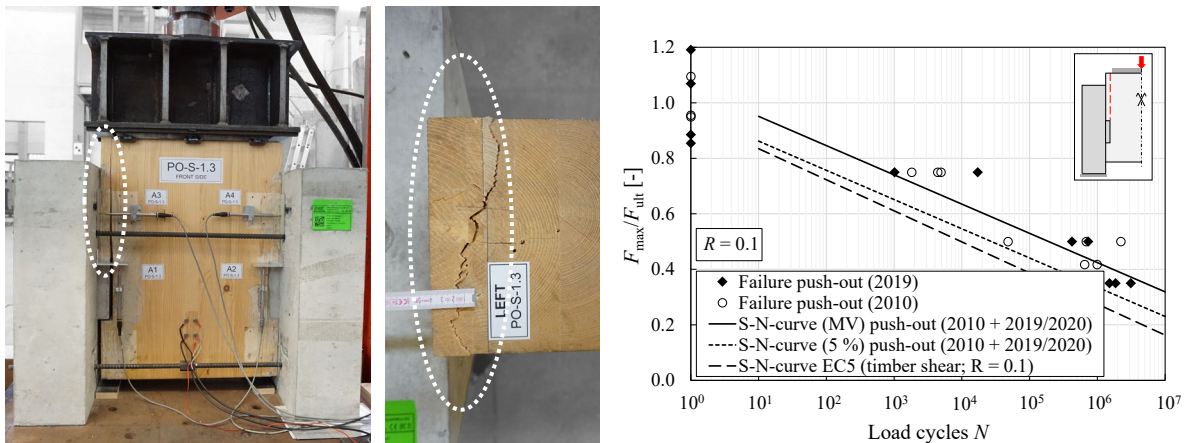


Figure 3: Push-out test specimen PO-S-1.3 after timber shear failure in front of the notch as front view (left), timber shear failure top view (middle) and S-N-curves for the stress ratio $R = 0.1$ derived from tests in 2019 and 2020 together with test results from Kuhlmann & Aldi (2010) [10] (right).

Figure 3 (right) shows the S-N-curve derived from the mean values (MV) of the tests for the relevant failure mode (timber shear failure) as well as the resulting statistically evaluated S-N-curve (5% fractile values). Both S-N-curves are located above the resulting S-N-curve for timber in shear according to EN 1995-2, A3 [9]. Therefore, the verification of the notches in shear according to the current rules seems to be on the safe side. Further information on the test evaluation and the statistical analysis can be found in [4], [6]. This confirms the already standardized fatigue verification given in [9] for timber in shear for a stress ratio of $R = 0.1$ also for the verification of the timber in front of the loaded edge of the notch in TCC systems.

Results obtained from cyclic push-out test series for a second stress ratio of $R = 0.4$, together with results obtained from TCC beam tests described in section 4, are shown as S-N-curves in Figure 8 (right). A stress ratio of $R = 0.4$ represents a typical stress ratio for TCC road bridges under traffic load in practice.

In addition, the verification that the fatigue rules are also applicable for real traffic by using the Palmgren-Miner Rule is still missing. Based on the cyclic test series with single amplitude load spectrum, mainly used to derive S-N-curves (series PO-C-2 and PO-C-5 in Figure 4 (right)), test series PO-C-6 was conducted with variable amplitude load spectrum (load protocol see Figure 4 (left)). A variable amplitude load protocol represents a more realistic scenario of recurring traffic loads on road bridges.

Figure 4 (right) shows that the linear interpolated mean value (corresponding to the linear damage accumulation hypothesis according to the Palmgren-Miner Rule [14]) is below the actual average of load cycles before failure in test series PO-C-6 and in this case on the safe side. However, this is only a single series of tests, which should not be considered as a complete validation of the Palmgren-Miner Rule for fatigue testing of timber, however, these test results give a positive indication. Further information on the evaluation of test series PO-C-6 can be found in [4], [6].

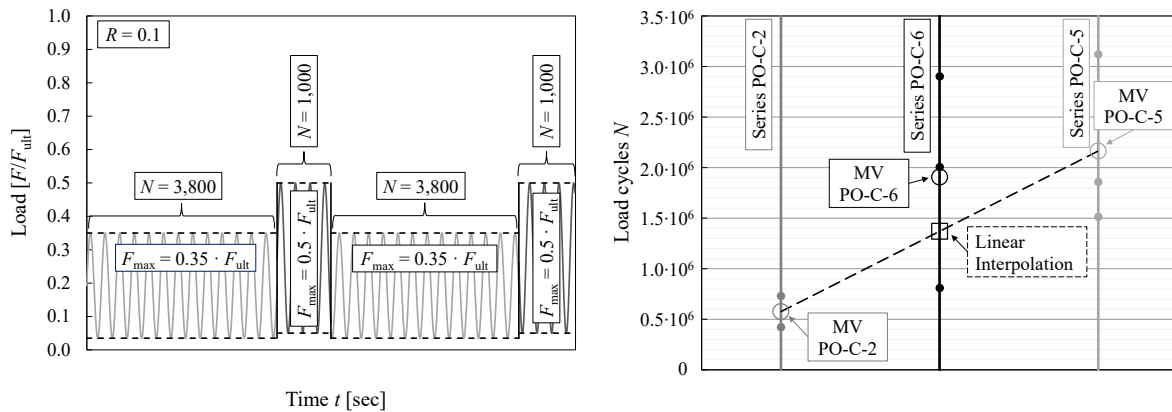


Figure 4: Load protocol of test series PO-C-6 with variable amplitude load spectrum (left) and comparison of the number of load cycles before failure of test series PO-C-6 with the results of test series PO-C-2 and PO-C-5 with comparable maximum load levels F_{max} conducted with single amplitude load spectrum (right).

4 TCC beam tests with stress ratio $R = 0.4$

4.1 Geometry, material and test programme

Based on the push-out test series, one static and two cyclic test series with a total of 9 tests on TCC beams (see Figure 5 and Figure 6) were conducted as 4 m long three-point bending tests at MPA, University of Stuttgart in 2021.

In comparison to push-out tests, the geometry of TCC beam test specimens is more similar to real TCC bridge constructions. Also, possible friction between timber and concrete can be simulated more realistically compared to push-out tests. As in practice, the timber elements in the area of the notches of both the push-out and the TCC beam test specimens were moisturized twice with water (30 min and 10 min before concreting the slab). However, there were no measurable differences in the influence of friction between the push-out and TCC beam tests. Initial adhesive friction break-off between timber and concrete was measurable, but similar for both test geometries and occurred at the beginning of the loading. Movable bearings were used for the TCC beam test setup to enable the TCC beam to move horizontally without restraint. As a single-span beam is purely governed by equilibrium, it can be assumed that the arrangement of only two notches (one on each side of the TCC beam) leads to evenly distributed forces to both notches. No strain gauges were used to measure the stress distribution on the beam, but for the range tested a linear elastic behaviour can be assumed.

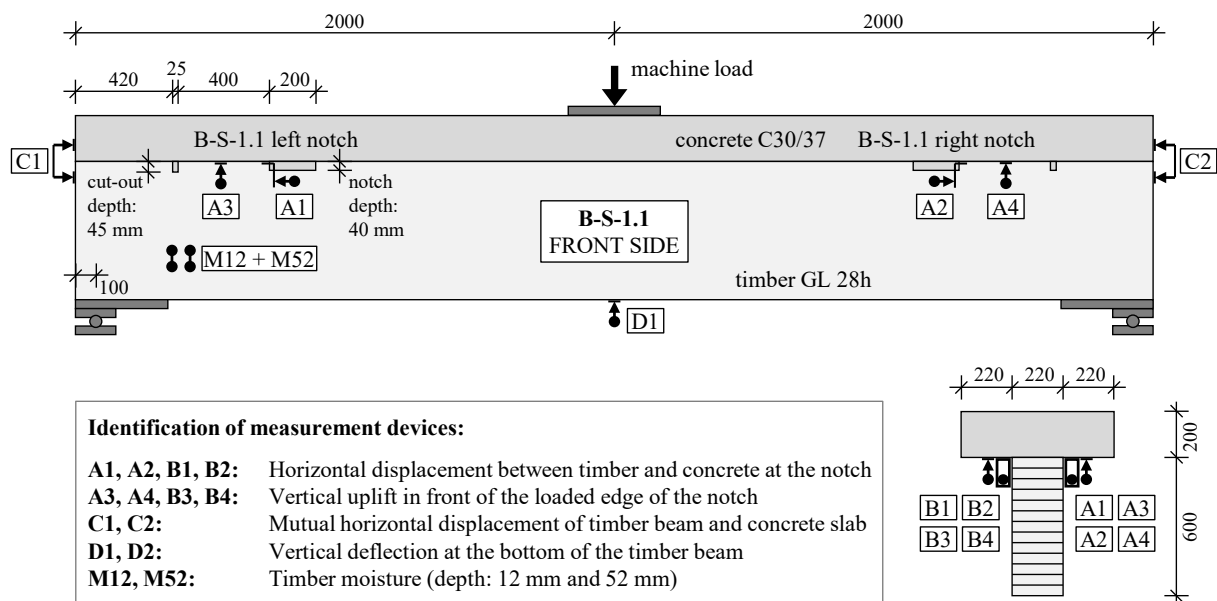


Figure 5: TCC beam test specimen with identification of measurement devices: front view (top) and cross section (bottom right), dimensions in mm [6].



The cyclic series were tested with a stress ratio of $R = 0.4$. These investigations aimed to confirm the results obtained from the push-out test series tested with the same stress ratio R and to derive even more accurate and meaningful S-N-curves based on the extended database.

The measurements of the notch, the timber length in front of the loaded edge of the notch and the material quality used are shown in Figure 5. They were similar to the push-out test specimens, already described in section 3. The TCC beams were manufactured in the same geometry as similar tests by Kuhlmann & Aldi (2010) [10], tested with a stress ratio of $R = 0.1$. The mean value of the carrying capacity F_{ult} determined from the static TCC beam tests of series B-S-1 was used as input value for determining the maximum loads F_{max} of the cyclic tests of series B-C-1 and B-C-2 (see Table 1).

Considering the maximum load F_{max} chosen in each case, the corresponding lower load F_{min} can be determined based on the stress ratio of $R = 0.4$. The resulting cyclic load protocol for the cyclic test series is shown in Figure 8 (left).

Table 1: Varied parameters of TCC beam test series conducted in 2021

Series No.	Tests	Stress ratio $R = \sigma_{min} / \sigma_{max}$	Frequency F [Hz]	Maximum load F_{max} [kN]
B-S-1	3	-	Static loading	-
B-C-1	3	0.4	2.5	$0.75 \cdot F_{ult}$
B-C-2	3	0.4	2.5	$0.60 \cdot F_{ult}$

4.2 Results of TCC beam tests and derived S-N-curves

For all TCC beam tests, the failure occurred as brittle timber shear failure in front of the loaded edge of the notch (see Figure 6). However, the first cyclic test of series B-C-2 with a relatively small maximum load of $F_{max} = 0.60 \cdot F_{ult}$ showed a long crack in the timber in front of the loaded edge of the notch after more than 6 million load cycles, but no brittle failure occurred. Considering a frequency of $F = 2.5$ Hz, this corresponds to a test period of more than 27 days.

For that reason, the maximum load was first increased to $0.65 \cdot F_{ult}$ and finally to $0.70 \cdot F_{ult}$ (see Figure 8 (left)) until, after a total of 7.19 million load cycles, a brittle timber shear failure in front of the loaded edge of the notch occurred. Therefore, the second test within this series was started with a maximum load of $0.65 \cdot F_{ult}$, which, however, only initiated failure after increasing the load to $0.70 \cdot F_{ult}$.

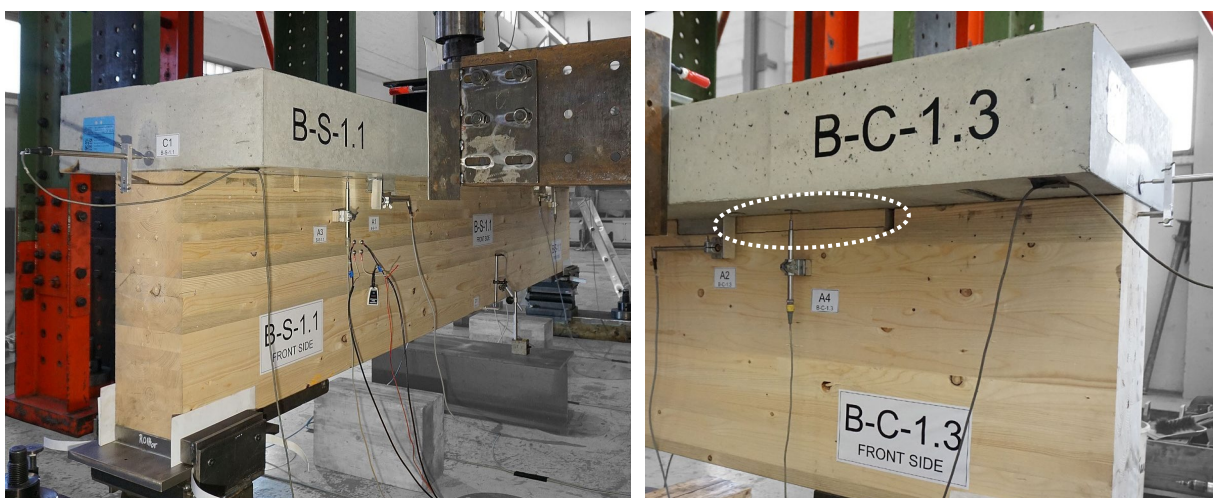


Figure 6: TCC beam specimen B-S-1.1 test setup at the MPA Stuttgart (left) and detail of the timber shear failure in front of the notch after cyclical loading of specimen B-C-1.3 (right).

Both run-outs could not be used for deriving the S-N-curves (but are shown in Figure 8 (left)). They confirm the tendency to high fatigue strength in the range of small maximum loads, as already observed by Simon [11]. Based on the results of the previous tests, the third test of series B-C-2 was finally started with a maximum load of $0.70 \cdot F_{ult}$. The failure occurred after 1.05 million load cycles. Thus, this test with single amplitude load spectrum could still be considered for the derivation of the S-N-curves with a stress ratio of $R = 0.4$.



All tests of series B-C-1 with a maximum load of $F_{max} = 0.75 \cdot F_{ult}$ failed at this load level (between $N = 71,880$ and $N = 516,980$ load cycles). Consequently, the results of series B-C-1 represent valuable input data for the S-N-curves derived in Figure 8 (right) based on all push-out and TCC beam tests with a stress ratio of $R = 0.4$. The measurement devices used for all TCC beam tests are marked at the respective locations in Figure 5. As an example, Figure 7 (right) shows the development in horizontal displacement at the notch for the corresponding side, where the brittle timber shear failure occurred.

All cyclic tests were first statically preloaded up to the mean load of the cyclic load protocol (shown in Figure 7 (left)). On average, the increase in displacement (between the start of cyclic loading and the brittle timber shear failure) was about 0.3 mm (see Figure 7 (right)).

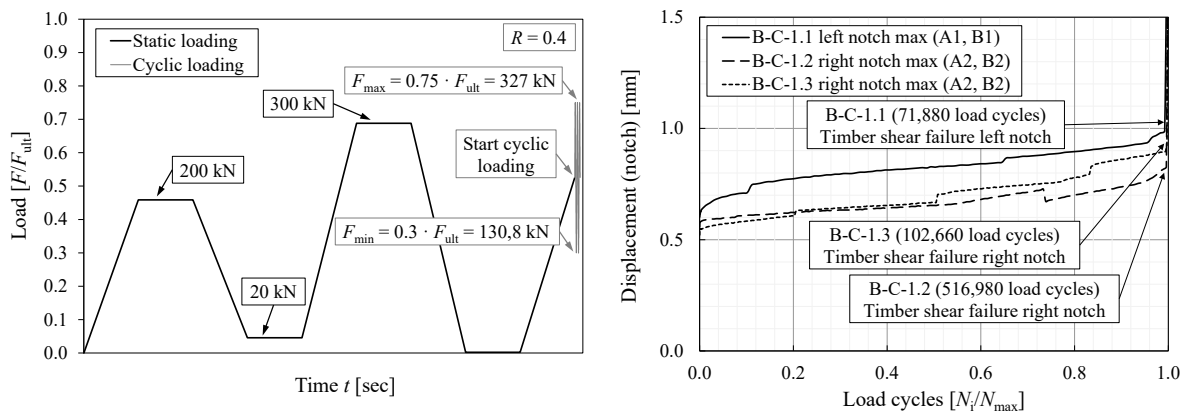


Figure 7: Static preloading together with the start of the cyclic loading for test series PO-C-1 (left) and horizontal displacement at the notch for all three tests of series B-C-1 (right).

Figure 8 (right) shows the S-N-curves derived from the mean values (MV) of the tests for the decisive failure mode (timber shear failure). In addition, the resulting statistically evaluated S-N-curves (5% fractile values) are shown as a combined evaluation of the TCC push-out and beam tests. This is shown in the same way for $R = 0.1$ in Figure 3 (right). For $R = 0.4$, the two S-N-curves are also above the resulting S-N-curve for timber in shear according to EN 1995-2, A.3 [9] and thus on the safe side.

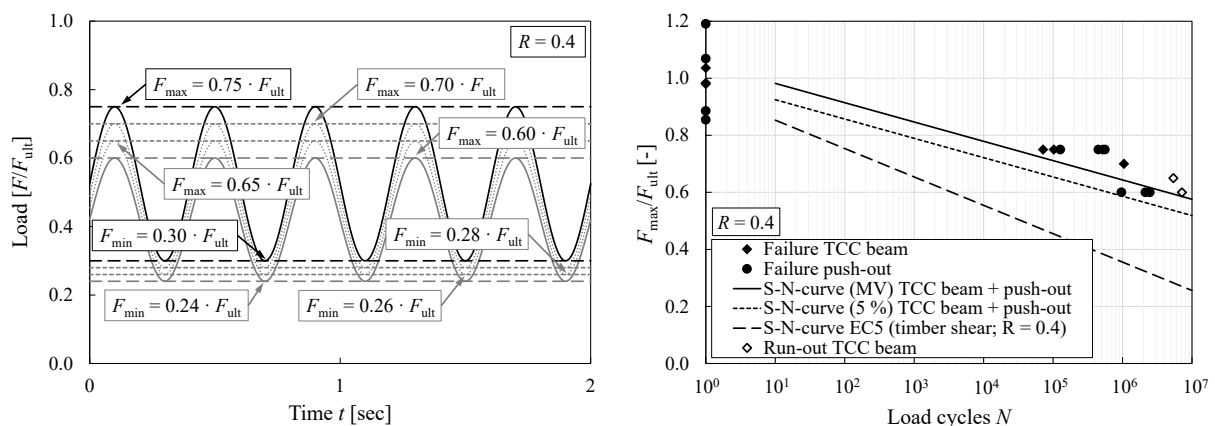


Figure 8: Load protocols of the cyclic loadings with a stress ratio of $R = 0.4$ (left) and S-N-curves for the stress ratio of $R = 0.4$ derived from TCC push-out and beam tests with marked run-outs (right).

A closer comparison shows that the distance between the S-N-curve derived from EN 1995-2, A.3 [11] and the S-N-curves derived from the tests with a stress ratio of $R = 0.4$ (Figure 8 (right)) is even larger than for the S-N-curves with $R = 0.1$ shown in Figure 3 (right). This indicates that the test results with a stress ratio of $R = 0.4$, which is more realistic in practice for TCC bridges, show an even higher fatigue strength compared to EN 1995-2, A.3 [9].



5 Summary and outlook

The discussed static and cyclic test series on TCC push-out and beam specimens with notched connections showed that the fatigue verification (decrease of strength by k_{fat}) for timber in shear, already implemented in EN 1995-2, A.3 [9], may also be applied with sufficient safety for the fatigue verification of notched connections in TCC bridges.

Within the future generation of the Eurocodes, the k_{fat} procedure will be maintained, but based now on a more elaborated background. Consequently, TCC-bridges with notched connections subjected to recurring traffic loads may be designed economically and safely. The spread of knowledge and a codification by the TS will allow for an increase in the use of sustainable timber constructions for bridges.

6 Acknowledgement

The investigations were funded by the German Research Foundation (DFG) – project number 397985109. This support is gratefully acknowledged.

We extend our appreciation to our DFG project partner, the Institute of Building Construction and Timber Structures at the Technical University of Braunschweig (Prof. Dr.-Ing. Mike Sieder and Peter Niebuhr, M.Sc.) for their very good cooperation.

Moreover, we thank SPAX International GmbH & Co. KG for providing screws for the specimens and MPA, University of Stuttgart for their great support in conducting the tests.

7 References

- [1] Gerold, M. (2007) Holzbrücken am Weg (in German). Self-published, ISBN: 978-3-00-023624-2, Karlsruhe, Germany.
- [2] Miebach F., Niewerth D., Wold F., Laraki J. (2018) Holz-Beton-Verbundbrücken – Erfahrungen und Perspektiven (in German). Qualitätsgemeinschaft Holzbrücken e.V.
- [3] CEN/TS 19103 (2021) Eurocode 5: Design of Timber Structures – Structural design of timber-concrete composite structures – Common rules and rules for buildings. Technical Specification, CEN European Committee for Standardization, November 2021.
- [4] Mönch S., Kuhlmann U. (2020) Fatigue Behaviour of Notched Connections for Timber-Concrete-Composite Bridges. In: International Network on Timber Engineering Research, INTER 2022, Online-conference, 17.-19. August 2020.
- [5] Kudla K. (2017) Kerven als Verbindungsmittel für Holz-Beton-Verbundstraßenbrücken (in German). Institute of Structural Design, University of Stuttgart, No. 2017-02, PhD thesis.
- [6] Mönch S. (2022) Performance of Notched Connections under Static and Cyclic Loading for Timber-Concrete Composite Systems. Institute of Structural Design, University of Stuttgart, PhD thesis, in preparation.
- [7] Kuhlmann U., Mönch S. (2018) Design Parameters of Notched Connections for TCC Structures as Part of Eurocode 5. In: International Network on Timber Engineering Research, INTER 2018, Tallinn, Estonia, 13.-16. August 2018.
- [8] Kuhlmann U., Sieder M., Mönch S., Niebuhr P. (2021) Ermüdungsverhalten von Kerven und selbstbohrenden Vollgewindeschrauben für die Anwendung als Verbindungsmittel bei Holz-Beton-Verbundträgern (Fatigue behaviour of notches and self-drilling screws for the application as connectors in TCC beams), (in German). University of Stuttgart, Institute of Structural Design and Technical University Braunschweig, Institute of Building Construction and Timber Structures, DFG-Research-Project, Project number: 397985109, 2018-2021.
- [9] EN 1995-2 (2004) Eurocode 5: Design of timber structures – Part 2: Bridges. European Committee for Standardization (CEN), Brussels.
- [10] Kuhlmann U., Aldi P. (2010) Fatigue strength of timber-concrete-composite bridges: Determination of a S-N-line for grooved connection and the “X-connector”. In: World Conference on Timber Engineering, WCTE, Trento, Italy, 20-24. June 2010.
- [11] Simon A. (2008) Analyse zum Trag- und Verformungsverhalten von Straßenbrücken in Holz-Beton-Verbundbauweise (in German). Bauhaus-Universität Weimar, PhD thesis.
- [12] EN 14080 (2013) Timber structures – Glued laminated timber and glued solid timber – Requirements. European Committee for Standardization (CEN), Brussels.
- [13] EN 1992-1-1 (2004) Eurocode 2: Design of concrete structures – Part 1-1: General rules and rules for buildings. European Committee for Standardization (CEN), Brussels with corrections and amendments + AC:2010.
- [14] Miner A. (1945) Cumulative Damage in Fatigue. In: Journal of Applied Mechanics 12 (1945), pp. 159-164.